Published in final edited form as:

Toxicol Appl Pharmacol. 2019 July 15; 375: 32–45. doi:10.1016/j.taap.2019.05.009.

Gadolinium-based contrast agents: stimulators of myeloid-induced renal fibrosis and major metabolic disruptors.

Catherine Do[1,2], **Bridget Ford**[2,3], **Doug Yoon Lee**[2], **Chunyan Tan**[2], **Patricia Escobar**[4], and **Brent Wagner**[4,5]

[1]South Texas Veterans Health Care System

[2]University of Texas Health Science Center at San Antonio

[3]University of the Incarnate Word

[4]Kidney Institute of New Mexico

[5]New Mexico Veterans Administration Health Care System

Abstract

Evidence for gadolinium-based contrast agent-(GBCA-) induced disease continues to mount. Risk factors for gadolinium-induced systemic fibrosis are entirely unexplored. Obesity-related renal injury is characterized by activation of glomerular mesangial cells and podocyte damage with alteration of lipid metabolism/lipid accumulation in both cell types resulting in matrix accumulation and eventual progression to glomerulosclerosis. We examined the consequences of GBCA treatment in the kidneys from mice with normal kidney function and the potential interplay between obesity and gadolinium exposure. We found that administration of GBCA (4 weeks) causes significant renal fibrosis and podocyte injury that are associated with metabolic disorders as evidenced by dyslipidemia. Metabolomic analysis demonstrated that renal lipid metabolism and metabolic markers of collagen turnover are significantly altered by gadolinium. GBCA stimulates myeloid-derived fibrocytes to the kidney. Obesity was induced by feeding a group of mice a high fat diet (HFD) for 22 weeks. Groups were sub-randomized to GBCA treatment versus none for 4 weeks before sacrifice. HFD-induced fibrosis and podocyte injury were worsened by GBCA. Similarly, HFD-mediated hyperlipidemia and lipid metabolites were exacerbated by gadolinium. This is the first evidence that GBCA causes significant metabolic disorders and kidney injury in mice without renal insufficiency and that the injurious actions of GBCA are amplified by obesity. The understanding of the functional interplay between gadolinium and obesity will allow the development of therapeutic interventions or the establishment of effective preventive measures to reduce gadolinium- and obesity-mediated renal pathologies.

Address for correspondence: Brent Wagner, Director, Kidney Institute of New Mexico, Chief, Renal Section, New Mexico Veterans Administration Health Care System, The University of New Mexico Biomedical Research Facility 323J, MSC04 2785, 1 University of New Mexico, Albuquerque, NM 87131.

Keywords

nephrogenic fibrosing dermopathy; chemokines; gadolinium; CCR2; fibrosis; bone marrow; renal insufficiency; antigens; CD45

INTRODUCTION

Magnetic resonance imaging is an important imaging modality necessary for medical diagnosis across multiple clinical settings. Gadolinium is a heavy rare earth element with unique paramagnetic properties rendering it ideally suited to enhance magnetic resonance images when administered intravenously in a pharmacologically-chelated form to reduce the extreme toxicity of the lanthanide (Reilly 2008). Gadolinium-based contrast agents have garnered a reputation as being well-tolerated— many, fallaciously, considering these to be biologically inert—and their use has risen to all-time highs as magnetic resonance imagers proliferate throughout the globe. Since these agents are practically wholly eliminated by renal excretion, the magnitude of their use can now be gauged by anthropogenic gadolinium pollution in surface waters and aquatic environments (Parant, Perrat et al. 2018).

Gadolinium-based contrast agents are far from biologically inert (Figure 1). In 2006, it was reported that these agents can trigger a profound and sometimes fatal systemic fibrosis (Grobner 2006). By 2014, it was realized that long-term gadolinium retention could be detected on unenhanced magnetic resonance imaging scans of the brain (Kanda, Ishii et al. 2014). Growing consumer concern prompted a meeting of the United States Food & Drug Administration Medical Imaging Drugs Advisory Committee on September 8, 2017 (FDA 2017) and subsequent prescriber information label changes warning of long-term gadolinium retention in vital organs following gadolinium-based contrast agent administration.

A common misperception is that gadolinium-based contrast agents are entirely eliminated by the kidney soon after intravenous administration; in reality, intravenous gadolinium-based contrast enters intermediate- and slow-release compartments (Hirano and Suzuki 1996) such as the cerebrospinal fluid within minutes (Nehra, McDonald et al. 2018). The result is that gadolinium can be retained in biological tissues for years (Wagner, Drel et al. 2016). Perhaps not coincidentally, gadolinium-induced systemic fibrosis can take years to manifest (Clases, Fingerhut et al. 2019). Gadolinium-based contrast is now being used in higher doses in chronically- and seriouslyill patients with variable renal function. Gadolinium-based contrast-induced *nephrotoxicity* has been described in patients and in animal models (Thomsen, Almen et al. 2002).

We conducted experiments to demonstrate that gadolinium-based contrast agent induces renal fibrosis. Gadolinium-based contrast agent treatment is known to induce systemic fibrosis with myeloid-derived fibrocytes as part of the disease (Wagner, Tan et al. 2012, Do, Barnes et al. 2014, Drel, Tan et al. 2016). To gauge myeloid involvement in this process, mice with partial nephrectomies (to model chronic kidney disease) underwent lethal irradiation followed by salvage bone marrow transplant from green fluorescent protein-expressing donors. Because renal disease is quite often the direct result of metabolic

disruption such as obesity, kidney metabolites were analyzed in a comparison of chow and high fat diet-fed mice sub-randomized to untreated and gadolinium-based contrast agent treatment. Our results are the first to demonstrate that gadolinium-based contrast agents ravage subcellular organelles and exert metabolic disruption on par of that with high fat diet-induced obesity.

MATERIAL AND METHODS

United States Food & Drug Administration Adverse Events Reporting System Public Dashboard.

Data were accessed in February, 2019. Terms of the search are listed in supplementary materials.

Animals.

All experimental protocols and procedures were in accorda nce with the Guide for the Care and Use of Laboratory Animals published by the National Institutes of Health and approved by the Institutional Animal Care and Use Committee. Endpoints were as previously reported (Wagner, Tan et al. 2012).

Bone marrow transplantation.

Female C57 black mice underwent 5/6 nephrectomy at 10–12 weeks. After 2 weeks acclimation, the mice were lethally-irradiated (950 rads divided into sessions spaced 4 hours apart, GammaCell 40, Atomic Energy of Canada Limited, Mississauga, ON, Canada). Bone marrow cells (1×10^7) were harvested from green fluorescent protein-expressing C57 black male mice (C57BL/6-Tg(CAG-EGFP)1310sb/LeySopJ, The Jackson Laboratory, Bar Harbor, ME) and administered via the tail veins. After 4 weeks for engraftment, animals were randomized into control ($n = 5$) or gadolinium contrast-treated groups (Omniscan, General Electric HealthCare, Little Chalfont, UK; 2.5 mmol/kg intraperitoneally, aiming for 20 doses over 4 weeks, $n = 6$). All experimental procedures and protocols were in accordance with the Guide for the Care and Use of Laboratory Animals published by the NIH and approved by the Institutional Animal Care and Use Committee (IACUC). Endpoints were 1) weight loss of 10%, 2) dermatologic findings previously described (Wagner, Tan et al. 2012), or 3) completion of 4 weeks of contrast treatment. Animals were examined daily for any signs of systemic fibrosis. At the time of sacrifice, dorsal skin thickness was measured in triplicate with digital calipers (VWR, Radnor, PA).

High fat diet.

Mice were randomized to a 60% saturated fat diet ($n = 20$) ad lib (20% protein, 20% carbohydrate, formula D12492, Research Diets, Inc., New Brunswick, NJ) for 22 weeks or control chow ($n = 20$). At 18 weeks of the diet, the groups were sub-randomized into untreated ($n = 10$) and gadolinium-based contrast agent-treated ($n = 10$) subgroups for 4 weeks.

Albuminuria.

Urinary albumin was measured from 24 hour collections with ELISA (Bethyl Laboratories, Inc., Montgomery, TX).

Tissue fixation, sectioning, and histology—The capsule was removed from the remnant kidne y followed by a butterfly section. A portion was fixed in 10% neutral-buffered formalin, and the cortex of the remnant was flash-frozen (for immunoblot, immunofluorescence, metabolomics, or gadolinium quantification).

Immunofluorescence—Paraffin-embedded tissue was sectioned on glass slides, deparaffinized in xylene, and re-hydrated. Sections of kidney (7 μm thick, paraffin-embedded as described in *Methods*) were stained for the indicated antigens followed by fluorescent secondary antibodies. Coverslips were adhered with mountant containing 4,6-diamidino-2-phenylindole (DAPI). Tissues were incubated with citric acid-based unmasking solution (Vector Laboratories, Burlingame, CA), blocked with bovine serum albumin (1%), goat serum (10%) in phosphate-buffered saline (pH 7.4) for 2 hours. For mouse antibodies, blocking was with a mouse on mouse immunodetection kit (Vector Laboratories, Burlingame, CA) per the manufacturer's instructions. Goat secondary antibodies to mouse and rabbit immunoglobulins were AlexaFluor594 and AlexaFluor488 (Thermo Fisher Scientific Life Sciences, Waltham, MA).

Metabolomics—A portion of kidney tissue (25 mg) was flash frozen in liquid nitrogen and transferred to polypropylene tubes. Samples were stored at −80°C until shipment to Metabolon (Morrisville, NC) for monoacylglycerol, diacylglycerol, and phospholipid metabolism.

Immunoblot—Tissue was homogenized in radioimmunoprecipitation assay buffer as previously described (Wagner, Tan et al. 2012, Do, Barnes et al. 2014). Primary antibodies were fibronectin, β actin, and alpha-smooth muscle actin (F3648, A2228, A5227 respectively; Sigma-Aldrich, St. Louis, MO) 1:3000, 1:2000, and 1:1000 respectively; GAPDH (sc-25778, Santa Cruz Biotechnology, Santa Cruz, CA) 1:1000; C-C chemokine receptor 2 (3415R, Biovision, Inc., San Francisco, CA); green fluorescent protein (ab290) 1:1000, (Abcam, Cambridge, MA).

Inductively-coupled plasma mass spectroscopy—Frozen tissues were processed by the Northwestern University Quantitative Bio-element Imaging Center. Tissue was transferred to metal-free tubes then dissolved with 1 mL 70% trace nitric acid and 100 μL trace hydrogen peroxide in a water bath at 70ºC for 12 hours. Digested samples, 200 μL, were transferred into metal-free tubes and diluted up to 5 mL with high-purity water (Millipore, Darmstadt, Germany). Samples were run through the inductively-coupled plasma mass spectrometer and compared with gadolinium-containing standards.

In vivo lysosomal integrity.

Serum-starved human foreskin fibroblasts were pre-treated with lucifer yellow 20 μM (Invitrogen) overnight, then treated with Omniscan 0.4 mM for 30 minutes. After washing,

photographs at 488 nm excitation, 519 nm emi ssion, treated with 0.2 mM gadolinium-based contrast. Confocal with lucifer yellow pre-staining, 40× objective 2× zoom, oil.

RESULTS

Mice were randomized by weight and treated with gadolinium-based contrast agent, 2.5 mmol/kg intraperitoneally daily, aiming for 20 doses over 4 weeks. Serum chemistries (collected at the endpoint) revealed increased creatinine in the gadolinium-treated group (Figure 2A). Gadolinium-based contrast agent treatment increased serum creatinine and decreased inverse creatinine; parameters that are highly specific for impaired glomerular filtration rate (particularly when detectable in mice). That the blood urea nitrogen level dropped in the gadolinium-based contrast agent group indicated a systemic and physiologic impact. Histologic analysis of the kidney cortices demonstrated mesangial expansion and tubular vacuolization in the gadolinium-treated group (Figure 2B, C). Furthermore, there were increases in mesangial and interstitial fibronectin, collagen, and the C-C chemokine receptor 2—a known mediator of gadolinium-based contrast agent-induced systemic fibrosis (Drel, Tan et al. 2016). Quantitatively, this receptor and fibronectin were increased in the renal cortex of the gadolinium-treated group (Figure 2D). Gadolinium content was increased in the renal cortices only in the gadolinium-based contrast agent-treated group (Figure 2E). Endpoint urinalysis also demonstrated an increase in albuminuria from the contrast-treated animals (personal communication, Dr. Yves Gorin, Ph.D.). Consistent with this, the number of podocytes was decreased as assessed by p57 and synaptopodin staining (Figure 2F). Metabolomic analysis on frozen kidney cortices demonstrated increased levels of extracellular matrix-relevant metabolites, trans-4-hydroxyproline and 5-(galactosylhydroxy)-L-lysine (Figure 2G). These data demonstrate that gadolinium-based contrast agents have a profound impact on renal function and histology.

The kidney is the primary reservoir for gadolinium-based contrast even days after a single dose (Kindberg, Uran et al. 2010). Given that the kidneys are a large and long-term reservoir for gadolinium-based contrast agents (Do, Barnes et al. 2014), renal cortex was examined for electron densities with electron microscopy (Figure 3A). Multiple electron densities were found within the glomerular mesangium and particularly within the vacuoles and juxtaposed to the mitochondria of the proximal tubules. High magnification revealed these electron dense nanostructures as aggregates, often spiculated, mesh-like, and ‘sea urchin’ shaped similar to what has been detected for rare earth elements, including gadolinium, in phagolysosomal-simulated solutions (Li, Ji et al. 2014). These electron densities were gadolinium-rich as assessed by scanning transmission electron microscopy equipped with energy-dispersive x-ray spectroscopy (Figure 3B).

We have demonstrated, in rats, that bone marrow-derived cells mediate gadolinium-based contrast agent-induced systemic fibrosis (Wagner, Tan et al. 2012). Mice with 5/6 nephrectomies (to model kidney disease) underwent lethal irradiation followed by salvage bone marrow transplantation from green fluorescent protein-(GFP-) expressing donors. After weeks of engraftment, the recipients were randomized to control and gadodiamide treatment (2.5 mmol/kg intraperitoneally, 5 doses per week for 4 weeks.

Fixed and paraffin-embedded sections of renal cortex were compared. Proximal tubules from the gadolinium-treated group universally demonstrated proximal tubular (isometric) vacuolization (Figure 4A). The glomeruli from the contrast-treated group demonstrated increased mesangial matrix (Figure 4B) Fibronectin expression was increased in the glomeruli from the gadolinium-treated group (Figure 4C). Fibronectin accumulation was evident in the renal cortex by immunofluorescent staining (Figure 4D) and immunoblot (Figure 4E). Quantitatively, the myeloid marker was elevated in the cortices from the gadolinium-based contrast agent-treated group (Figure 4F). CD45RO is a marker for myeloid-derived fibrocytes and may, at some point, be a biomarker for gadolinium-based contrast agent-induced systemic fibrosis (Pilling, Fan et al. 2009). Renal cortex from the gadolinium-treated groups demonstrated more myeloid infiltration in the glomeruli and the interstitium in addition to elevated (and co-expressed) CD45RO (Figure 4G). These data demonstrate, again, that gadolinium-based contrast agents exert profound histologic effects in the kidney and induce the recruitment of myeloid-derived cells, possibly fibrocytes, into the tissue.

Despite a common misconception among clinicians and diagnosticians, gadolinium-based contrast agents are not inert substances (Bellin and Van Der Molen 2008). The effect of gadolinium-based contrast agent treatment on the metabolic profile of the kidney was examined in contrast treated mice with normal renal function (Figure 5). (This allowed determination of whether pre-existing chronic kidney disease was requisite for gadolinium-based contrast agent-induced systemic fibrosis or not *and* provided a baseline to gauge the similarity with high fat diet-induced kidney fibrosis with that induced by gadolinium and the impact of the combination.) Multiple metabolites were altered from the control in several pathways, including glycolysis (Figure 5A), the tricarboxylic acid cycle (Figure 5B), and mitochondrial respiration (Figure 5C). In total, gadolinium-based contrast agent treatment profoundly increased renal glycolysis, increased lactate production, and increased the anaplerotic reaction intermediates— citrate, malate, α-ketoglutarate—consistent with *impaired* oxidative phosphorylation.

Gadolinium-based contrast agents were found to have profound dyslipidemic effects by the endpoint of the study (Figure 6A). Metabolomic analysis of the renal cortices demonstrated alterations in phospholipid metabolism (Figure 6B), monoacylglyceride and diacylglyceride pathways (Figure 6C), and the composition of the cellular and subcellular lipids (Figure 6D). Provided the evidence of gadolinium-rich crystalline nanostructure formation, and the disruption of lysosomal membranes (Figure 3) these data demonstrate that gadolinium-based contrast agents *impacts homeostatic quality control in vivo.*

Since gadolinium-based contrast agent treatment was far from inert physiologically and metabolically, and as the profiles resemble that of metabesity, another condition associated with the promotion of fibrosis, a head-to-head comparison of the effects of gadolinium-based contrast (20 doses over 20 weeks) on a control, chow diet on week18 of the 22-week long high-fat diet (60% kcal saturated fat). Although both gadolinium-based contrast agent treatment and high fat-induced obesity induced mesangial sclerosis and interstitial fibrosis (Figure 7A), these effects were augmented by the combination of high fat and gadolinium. The impact on fibrosis and α-smooth muscle actin expression, a marker of activated

myofibroblasts (Tomasek, Gabbiani et al. 2002), were quantitatively greater in the high fat-induced obesity group that received gadolinium-based contrast agent (Figure 7B). Similarly, the serum lipid profiles (Figure 7C), and insulin concentrations were all amplified in the high fat diet group by the additional treatment with gadolinium-based contrast agents. In order to detect the abnormal accumulation of fat in the experimental groups, renal cortices were analyzed histologically after oil red O staining (Figure 7D). Both glomeruli and proximal tubule demonstrated lipid-laden deposits. Importantly, this same phenomenon was present in the cortices from gadolinium-based contrast agent-treated animals that were on normal chow diets. The effect was augmented with the combination of high fat diet-induced obesity and gadolinium treatment. These data, in total, suggest that the mechanisms of fibrosis are by complementary mechanisms.

Renal cortex was examined using transmission electron microscopy (Figure 8). The proximal tubules from the high fat diet, the chow diet with gadolinium treatment, and the high fat diet-induced obesity with gadolinium-based contrast agent treatment all demonstrated a high degree of proximal tubule vacuolization. Only the vacuoles from the gadolinium treatment groups demonstrated the electron-dense nanowire deposits, often with lysosomal membranic disruption, and with the gadolinium often in the vicinities of mitochondria (Figure 8A). The glomerular basement membranes were similarly compared among these groups (Figure 8B), with evidence of progressive podocyte effacement in the experimental groups.

To determine if the mechanisms for gadolinium- and obesity-induced renal fibrosis are complementary, a number of kidney metabolites were compared among the experimental groups (Figure 9). The amplitude of derangement when the obese group received gadolinium-based contrast agent was consistent for the representative metabolites for the monoacylglycerol, diacylglycerol, and phospholipid pathways (Figure 9A). Similar perturbations (invariably in the same direction) were detected for metabolites from glycolysis (Figure 9B), the tricarboxylic acid cycle (Figure 9C), and mitochondrial respiration (Figure 9D). Gadolinium-based contrast agent treatment in the chow diet group had a profound impact in multiple metabolic pathways, something that would have not been predicted based on an assumption that these are inert agents. The pro-fibrotic properties of gadolinium-based contrast agents are not only similar to what can be induced by experimental obesity, but the two have a complementary tendency to amplify the severities of the pathology.

Because compromised lysosomal integrity was detected in each of the gadolinium-based contrast agent-treated groups, and as this may be a common mechanism with metabesity, a prospective *in vitro* experiment using cultured human fibroblasts was conducted. Cells were incubated with the lysosomal dye, lucifer yellow, overnight and washed, followed by a short incubation with gadolinium-based contrast (with clinically-relevant concentration). Within 30 minutes, enlarged, dense, and granular lysosomal patterns were evident in the gadolinium-treated cells (Figure 10). In total, these data not only demonstrate that gadolinium-based contrast agents are far from inert substances, but indicate that these lead to the formation of crystalline nanostructures, disrupt lysosomal integrity, and profoundly impact mitochondrial function in a manner similar to obesity.

DISCUSSION

Gadolinium-based contrast agents have been reported to be nephrotoxic in humans (Kaufman, Geller et al. 1999, Spinosa, Angle et al. 2000, Schenker, Solomon et al. 2001), particularly in the setting of diabetes (Gemery, Idelson et al. 1998, Akgun, Gonlusen et al. 2006). In a rabbit model, the gadolinium-based contrast agent gadopentetate induced high urinary concentration of the brush-border proteins leucine aminopeptidase, alkaline phosphatase, and gamma glutamyl transferase *and* a lysosomal marker of general renal damage, N-acetyl β-D-glucosaminidase (Leander, Allard et al. 1992). These direct measures of *nephron damage were detectable within one hour of contrast administration.*

Prompted by gadolinium retention in the brain, in 2017 the European Medicines Agency recommended suspending marketing authorization for an entire class of gadolinium-based pharmacologic agents. For this reason and the known retention of gadolinium in multiple other body organs in patients (regardless of renal function), the clustering of symptoms reported to the Food & Drug Administration Ad verse Event Reporting System correlating with these agents, and concern by numerous patients the United States Food & Drug Administration voted to add a warning to the labels of all gadolinium-based contrast agents on September 8, 2017 (Reddy 2017). Chronic adverse effects from gadolinium-based contrast agents in patients with normal kidney function may be a harbinger that these are a continuum with NSF.

Knowing the clinical impact of biologically-active rare earth metals, such as gadolinium, is critical given the ubiquity of their use and potential for irreversible patient harm (Leyba and Wagner 2019). Few studies have examined the effects of gadolinium-based contrast in mice. Our study successfully duplicates gadolinium-based contrast agent-induced fibrosis in the mouse and provides an excellent method of myeloid lineage tracing. Our results demonstrate that mice—regardless of renal function— treated with gadolinium-based contrast demonstrate renal (glomerular and interstitial) fibrosis. The study also provides a large mechanistic insight about common pathways induced by gadolinium-based contrast agents and metabolic disruptions such as obesity.

The risk for systemic fibrosis, like every malady that accompanies progressive renal insufficiency, likely follows a curvilinear pattern. Other than renal insufficiency and gadolinium exposure, there are no other robust risk factors for nephrogenic systemic fibrosis. *Not all end-stage renal disease patients exposed to gadolinium develop terminal systemic fibrosis* (Wagner, Drel et al. 2016). Therefore, *there are other lurking risk factors for gadolinium-induced disease.* The symptoms and signs of gadolinium-induced systemic fibrosis are similar to many sclerotic disorders, but the distribution of findings and histology are unique. In scleredema diabeticorum (diabetic thick skin), much of the dermal histology resembles what has been described in gadolinium-associated dermal fibrosis, i.e., large and disorganized collagen bundles, mucopolysaccharides, and active fibroblasts (Hanna, Friesen et al. 1987).

Cationic lanthanum (gadolinium is a lanthanide heavy rare earth metal) will bind to mitochondrial membranes and can enter mitochondrial matrix (Piccinini, Meloni et al.

1975). Metabolic activity of neuronal mitochondria is disrupted within 3 hours of exposure to $GdCl_3$ (Feng, Xia et al. 2010). Direct treatment of isolated mitochondria with 100–500 μM gadolinium (III) led to ultrastructural changes, including swelling (Zhao, Zhou et al. 2014).

Our research team was the first to report the *in vivo* formation of crystalline, mesh-like nanostructures within skin and renal cells (Wagner 2017). These structures are identical to those that form in phagolysosomal-simulated solutions (Li, Ji et al. 2014). *These sea urchin-shaped anomalies resemble how rare earth elements leach phosphates out of bacterial membranes* (Dr. Kimberly Butler, Ph.D., Sandia National Laboratories, personal communication). Our study provides the first mechanistic process in the initiation of gadolinium-based contrast agent-induced disease.

The **metabolomic profiling** of kidney tissue from gadolinium-based contrast agent-treated animals, the high fat diet-induced obese group, and the combination of the two represent important *mechanistic* discoveries. Gadolinium-based contrast agents—often inappropriately assumed to be inert—*increased glycolysis* (Figure 5a), similar to what has been found in cancerous cells (Porporato, Dhup et al. 2011). Concomitantly, gadolinium-based contrast—proven biologically-active substances (Wagner, Tan et al. 2012, Do, Barnes et al. 2014, Drel, Tan et al. 2016, Wagner, Drel et al. 2016, Do, Drel et al. 2019, Leyba and Wagner 2019)—*dysregulate* energy production in the cortex. Citrate was elevated in the tissue, yet the glycolytic intermediates were suppressed with an elevation of lactate, suggesting that oxidative phosphorylation is impaired (Figure 11). This deficiency is consistent with the increases of the tricarboxylic acid intermediates (Figure 5B), and the relative paucity of phosphate (Figure 5C). If a lanthanide can leach phosphates from the lysosomal membranes — consistent with the formation of the sea urchin-shaped crystalline nanostructures (Figure 3) that have been demonstrated *in vitro* ((Li, Ji et al. 2014) and Dr. Kimberly Butler, Ph.D., Sandia National Laboratories, personal communication)—then *perturbation of energy production* by *cellular depletion of phosphates* is an attractive mechanism. Choline, the precursor to acetyl-CoA, is reduced (Figure 6B); again, supporting that gadolinium-based contrast agents pervert normal cellular function. Phosphoethanolamine elevation is *consistent with the hypothesis* that *there is phospholipid breakdown* (Figure 6B). Gadolinium-based contrast agent administration—a practice that has been inappropriately assumed to be biologically inconsequential—elevated kidney monoacylglycerols and diacylglycerols, such as stearoyl-arachidonoyl-glycerol (18:0/20:4)—a marker noted in viscerally-obese patients with the metabolic syndrome (Candi, Tesauro et al. 2018). That all of these metabolites are altered *in the same direction* by gadolinium-based contrast agent administration and high fat diet-induced obesity, *and* that the combination often *amplified the aberrancies* (Figure 9) demonstrates a central and profound metabolic mediator of fibrosis by these two very different stimuli. Histologically, the commonality lies with proximal tubule vacuolization—engorged lysosomes—and subsequent subcellular violence that ends with the ravaging of a vital organ.

Gadolinium-based contrast agent-induced adverse effects are entirely a man-made disease. Contemporary medicine cannot revoke its responsibility for complications that occur from the intravenous administration of non-physiologic rare earth metals. Translational scientists

are obliged not to be indifferent to patients with gadolinium retention or systemic fibrosis. Medical and environmental research cannot divest itself of the responsibility for understanding how retained gadolinium elicits pathologic effects. Risk is the product of consequence and probability. The consequence of an incurable, chronically painful, and debilitating disorder eclipses the probability of acquiring gadolinium-based contrast agent-induced toxicity with regularity in our clinics and hospitals. We demonstrate that gadolinium-based contrast agents vandalize subcellular organelles and subvert normal mitochondrial function in the kidney in manner akin to common conditions, such as obesity. These discoveries will help break the vicious cycle in which gadolinium-based contrast agent exposure in patients with normal kidney function or in obese patients lend to the susceptibility to gadolinium-mediated renal pathologies.

Supplementary Material

Refer to Web version on PubMed Central for supplementary material.

ACKNOWLEDGEMENTS

This work is dedicated to Dr. Yves Gorin, Ph.D. (1967–2018). The research was funded by the Veterans Administration Merit Award (I01 BX001958, BW); the National Institutes of Health through Grants R01 DK-102085 (BW). The corresponding author serves as a consultant for a firm representing patients with gadolinium-based contrast agent-induced adverse effects.

REFERENCES

Akgun H, Gonlusen G, Cartwright J Jr., Suki WN and Truong LD (2006). “Are gadolinium-based contrast media nephrotoxic? A renal biopsy study.” Arch Pathol Lab Med 130(9): 1354–1357. [PubMed: 16948524]

Bellin MF and Van Der Molen AJ (2008). “Extracellular gadolinium-based contrast media: an overview.” Eur J Radiol 66(2): 160–167. [PubMed: 18358659]

Candi E, Tesauro M, Cardillo C, Lena AM, Schinzari F, Rodia G, Sica G, Gentileschi P, Rovella V, Annicchiarico-Petruzzelli M, Di Daniele N and Melino G (2018). “Metabolic profiling of visceral adipose tissue from obese subjects with or without metabolic syndrome.” Biochem J 475(5): 1019–1035. [PubMed: 29437994]

Clases D, Fingerhut S, Jeibmann A, Sperling M, Doble P and Karst U (2019). “LA-ICP-MS/MS improves limits of detection in elemental bioimaging of gadolinium deposition originating from MRI contrast agents in skin and brain tissues.” J Trace Elem Med Biol 51: 212–218. [PubMed: 30466933]

Do C, Barnes JL, Tan C and Wagner B (2014). “Type of MRI contrast, tissue gadolinium, and fibrosis.” Am J Physiol Renal Physiol 307(7): F844–855. [PubMed: 25100280]

Do C, Drel V, Tan C, Lee DY and Wagner B (2019). “‘Nephrogenic’ systemic fibrosis is mediated by myeloid C-C chemokine receptor 2 (accepted 3/27/2019, Journal of Investigative Dermatology)”

Drel VR, Tan C, Barnes JL, Gorin Y, Lee DY and Wagner B (2016). “Centrality of bone marrow in the severity of gadolinium-based contrast-induced systemic fibrosis.” FASEB J 30(9): 3026–3038. [PubMed: 27221979]

FDA. (2017). “Medical Imaging Drugs Advisory Committee Meeting. Gadolinium retention after gadolinium based contrast magnetic resonance imaging in patients with normal renal function. Briefing document”, from https://www.fda.gov/downloads/AdvisoryCommittees/CommitteesMeetingMaterials/Drugs/MedicalImagingDrugsAdvisoryCommittee/UCM572848.pdf.

Feng X, Xia Q, Yuan L, Yang X and Wang K (2010). “Impaired mitochondrial function and oxidative stress in rat cortical neurons: implications for gadolinium-induced neurotoxicity.” Neurotoxicology 31(4): 391–398. [PubMed: 20398695]

Gemery J, Idelson B, Reid S, Yucel EK, Pagan-Marin H, Ali S and Casserly L (1998). "Acute renal failure after arteriography with a gadolinium-based contrast agent." AJR Am J Roentgenol 171(5): 1277–1278. [PubMed: 9798860]

Grobner T (2006). "Gadolinium--a specific trigger for the development of nephrogenic fibrosing dermopathy and nephrogenic systemic fibrosis?" Nephrol Dial Transplant 21(4): 1104–1108. [PubMed: 16431890]

Hanna W, Friesen D, Bombardier C, Gladman D and Hanna A (1987). "Pathologic features of diabetic thick skin." J Am Acad Dermatol 16(3 Pt 1): 546–553. [PubMed: 3819098]

Hirano S and Suzuki KT (1996). "Exposure, metabolism, and toxicity of rare earths and related compounds." Environ Health Perspect 104 Suppl 1: 85–95. [PubMed: 8722113]

Kanda T, Ishii K, Kawaguchi H, Kitajima K and Takenaka D (2014). "High signal intensity in the dentate nucleus and globus pallidus on unenhanced T1-weighted MR images: relationship with increasing cumulative dose of a gadolinium-based contrast material." Radiology 270(3): 834–841. [PubMed: 24475844]

Kaufman JA, Geller SC, Bazari H and Waltman AC (1999). "Gadolinium-based contrast agents as an alternative at vena cavography in patients with renal insufficiency--early experience." Radiology 212(1): 280–284. [PubMed: 10405754]

Kindberg GM, Uran S, Friisk G, Martinsen I and Skotland T (2010). "The fate of Gd and chelate following intravenous injection of gadodiamide in rats." Eur Radiol 20(7): 1636–1643. [PubMed: 20157815]

Leander P, Allard M, Caille JM and Golman K (1992). "Early effect of gadopentetate and iodinated contrast media on rabbit kidneys." Invest Radiol 27(11): 922–926. [PubMed: 1464511]

Leyba K and Wagner B (2019). "Gadolinium-based contrast agents: why nephrologists need to be concerned." Curr Opin Nephrol Hypertens 28(2): 154–162. [PubMed: 30531473]

Li R, Ji Z, Chang CH, Dunphy DR, Cai X, Meng H, Zhang H, Sun B, Wang X, Dong J, Lin S, Wang M, Liao YP, Brinker CJ, Nel A and Xia T (2014). "Surface interactions with compartmentalized cellular phosphates explain rare earth oxide nanoparticle hazard and provide opportunities for safer design." ACS Nano 8(2): 1771–1783. [PubMed: 24417322]

Nehra AK, McDonald RJ, Bluhm AM, Gunderson TM, Murray DL, Jannetto PJ, Kallmes DF, Eckel LJ and McDonald JS (2018). "Accumulation of Gadolinium in Human Cerebrospinal Fluid after Gadobutrol-enhanced MR Imaging: A Prospective Observational Cohort Study." Radiology 288(2): 416–423. [PubMed: 29737947]

Parant M, Perrat E, Wagner P, Rosin C, Py JS and Cossu-Leguille C (2018). "Variations of anthropogenic gadolinium in rivers close to waste water treatment plant discharges." Environ Sci Pollut Res Int

Piccinini F, Meloni S, Chiarra A and Villani FP (1975). "Uptake of lanthanum by mitochondria." Pharmalogical Research Communications 7(5): 429–435.

Pilling D, Fan T, Huang D, Kaul B and Gomer RH (2009). "Identification of markers that distinguish monocyte-derived fibrocytes from monocytes, macrophages, and fibroblasts." PLoS One 4(10): e7475. [PubMed: 19834619]

Porporato PE, Dhup S, Dadhich RK, Copetti T and Sonveaux P (2011). "Anticancer targets in the glycolytic metabolism of tumors: a comprehensive review." Front Pharmacol 2: 49. [PubMed: 21904528]

Reddy S (2017). A question for anyone getting an MRI. The Wall Street Journal New York, Dow Jones & Company CCLXX: 2.

Reilly RF (2008). "Risk for nephrogenic systemic fibrosis with gadoteridol (ProHance) in patients who are on long-term hemodialysis." Clin J Am Soc Nephrol 3(3): 747–751. [PubMed: 18287249]

Schenker MP, Solomon JA and Roberts DA (2001). "Gadolinium arteriography complicated by acute pancreatitis and acute renal failure." J Vasc Interv Radiol 12(3): 393. [PubMed: 11287523]

Spinosa DJ, Angle JF, Hagspiel KD, Kern JA, Hartwell GD and Matsumoto AH (2000). "Lower extremity arteriography with use of iodinated contrast material or gadodiamide to supplement CO2 angiography in patients with renal insufficiency." J Vasc Interv Radiol 11(1): 35–43. [PubMed: 10693711]

Thomsen HS, Almen T, Morcos SK and Contrast R Media Safety Committee Of The European Society Of Urogenital (2002). "Gadolinium-containing contrast media for radiographic examinations: a position paper." Eur Radiol 12(10): 2600–2605. [PubMed: 12271402]

Tomasek JJ, Gabbiani G, Hinz B, Chaponnier C and Brown RA (2002). "Myofibroblasts and mechano-regulation of connective tissue remodelling." Nat Rev Mol Cell Biol 3(5): 349–363. [PubMed: 11988769]

Wagner B (2017). ""The pathophysiology and retention of gadolinium."." United States Food & Drug Administration Medical Imaging Drugs Advisory Committee: 1–23.

Wagner B, Drel V and Gorin Y (2016). "Pathophysiology of gadolinium-associated systemic fibrosis." Am J Physiol Renal Physiol 311(1): F1–F11. [PubMed: 27147669]

Wagner B, Tan C, Barnes JL, Ahuja SS, Davis TL, Gorin Y and Jimenez F (2012). "Nephrogenic systemic fibrosis: Evidence for bone marrow-derived fibrocytes in skin, liver, and heart lesions using a 5/6 nephrectomy rodent model." Am J Pathol 181(6): 1941–1952. [PubMed: 23041060]

Zhao J, Zhou ZQ, Jin JC, Yuan L, He H, Jiang FL, Yang XG, Dai J and Liu Y (2014). "Mitochondrial dysfunction induced by different concentrations of gadolinium ion." Chemosphere 100: 194–199. [PubMed: 24321333]

- Gadolinium-based contrast agents are not biologically inert; in our model, magnetic resonance imaging contrast agent treatment impaired renal function, induced pathologic damage, and increased kidney fibrosis.
- Mesh-like, electron-dense, gadolinium-rich nanostructures form in the renal glomerulus and proximal tubule as a result of magnetic resonance imaging contrast agent administration; the resultant subcellular violence results in recruitment of myeloid-derived fibrocytes and dysregulation of cellular energy production.
- Gadolinium-based contrast agent treatment induces dyslipidemia (elevated total cholesterol, elevated triglycerides) and induces insulin resistance; analogous to high fat diet-induced obesity, gadolinium-based contrast agents promote accumulation of lipid-laden deposits in the kidney.
- Histologic damage induced by gadolinium-based contrast agent treatment and experimental obesity are similar (and additive); obesity and gadolinium-based contrast agent treatment disrupt cellular metabolism in similar manners (with respect to disrupted oxidative phosphorylation, glycolytic switching, and perturbation of the tricarboxylic acid cycle).
- Despite low systemic concentrations, gadolinium from magnetic resonance imaging contrast is retained and aggregates in the lysosomes of vital organs, such as the kidneys; this process—similar to how lanthanum cations leach phosphorous from cellular membranes—induces the disruption of normal cellular metabolism that culminates in the initiation of fibrosis.

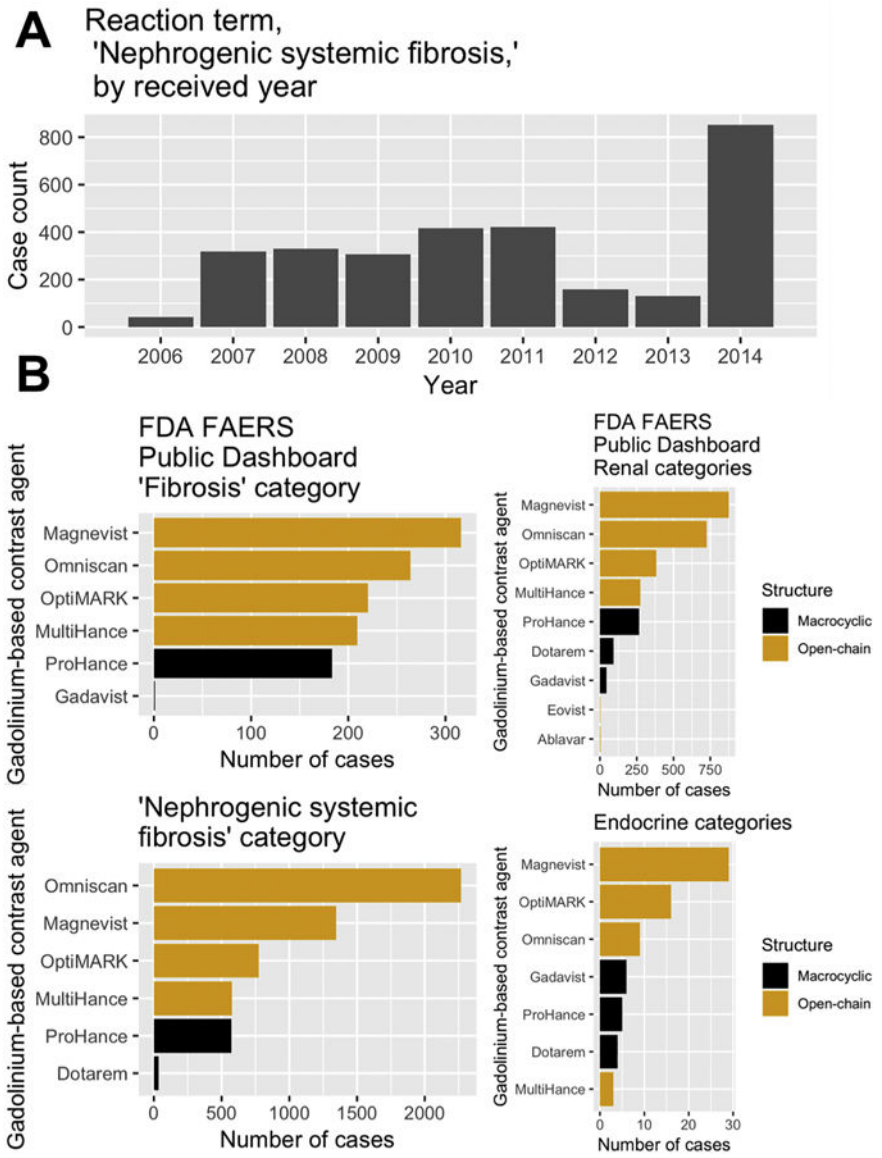

Figure 1.

United States Food & Drug Administration Adverse Events Reporting System (FAERS) data for gadolinium-based contrast agents. **A.** Case counts for the reaction term “nephrogenic systemic fibrosis” by received year. The total number, as of this writing, is 3,091. **B.** Multiple brands of gadolinium-based contrast agents, despite having different market shares, have overlapping reports of reactions: ‘fibrosis,’ ‘nephrogenic systemic fibrosis,’ renal disorders, and endocrine disorders.

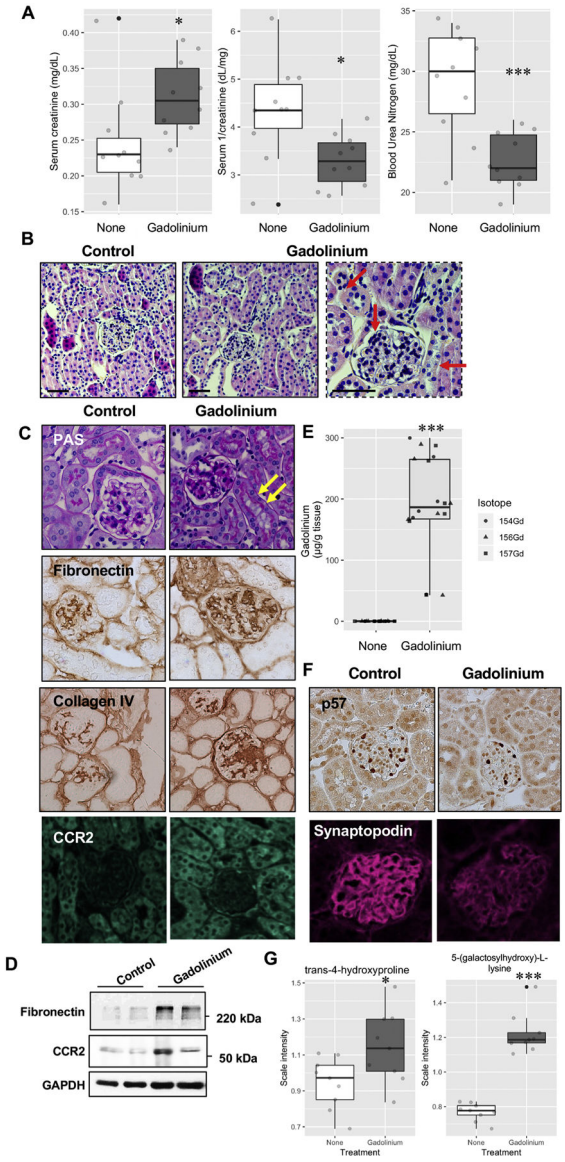

Figure 2.

Gadolinium impairs renal function conco mitant with pathologic changes in the kidney. **A.** Plasma was obtained from untreated and contrast-treated (2.5 mmol/kg intraperitoneally, 20 doses over 4 weeks) mice *without renal insufficiency* at the endpoint. **B.** Gadolinium-based contrast agents induce proximal tubular vacuolization, mesangial hypercellularity, and tubular damage (arrows). H&E, calibration bars = 0.05 mm. **C.** Glomerular pathology in gadolinium-treated mice. Arrows indicate proximal tubular vacuolization. PAS, immunohistochemistry for fibronectin, immunohistochemistry for collagen type IV, and immunofluorescence for CCR2; 400 _. **D.** Gadolinium induces elevated fibronectin and CCR2 in the renal cortex. Immunoblot. **E.** Treated mice demonstrated the accumulatio n of gadolinium. Inductively-coupled plasma mass spectroscopy. **F.** The effect of gadolinium on the podocyte markers p57 (immunohistochemical stain) and synaptopodin (immunofluorescence); 400 _. **G.** Biomarkers derived from metabolomic assay of flash-

frozen kidney tissue from untreated and gadolinium (Gd) -treated groups, n = 9 each. Boxes represent upper and lower quartile limits, + mean, —— median, whiskers the maximum and minimum of the distribution, *, $P < 0.05$, *** $P < 0.001$ by *t*-test.

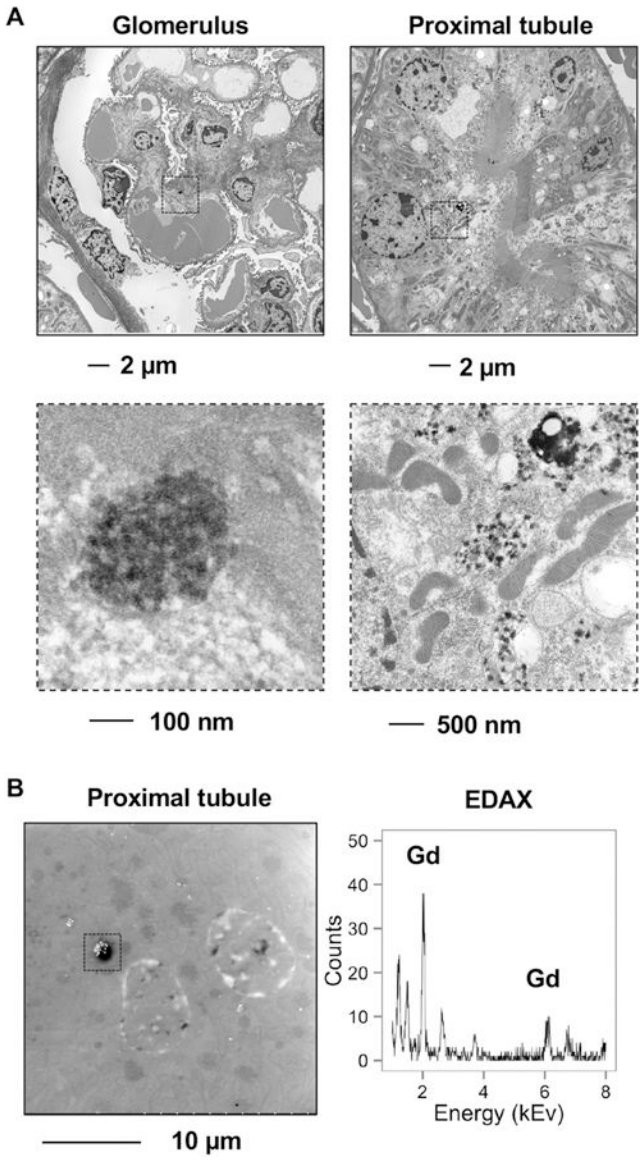

Figure 3.

A. (Left) Electron-dense deposits pepper the glomerular mesangium. (Right) In the proximal tubule, these electron-dense mesh-like nanowire structures are found in the proximity of mitochondria which were dense, elongated, and fissioning. **B.** Scanning electron microscopy of the proximal tubular electron-dense deposits with energy-dispersive x-ray spectroscopy (EDAX) revealed gadolinium. Calibration bar, 10 μm.

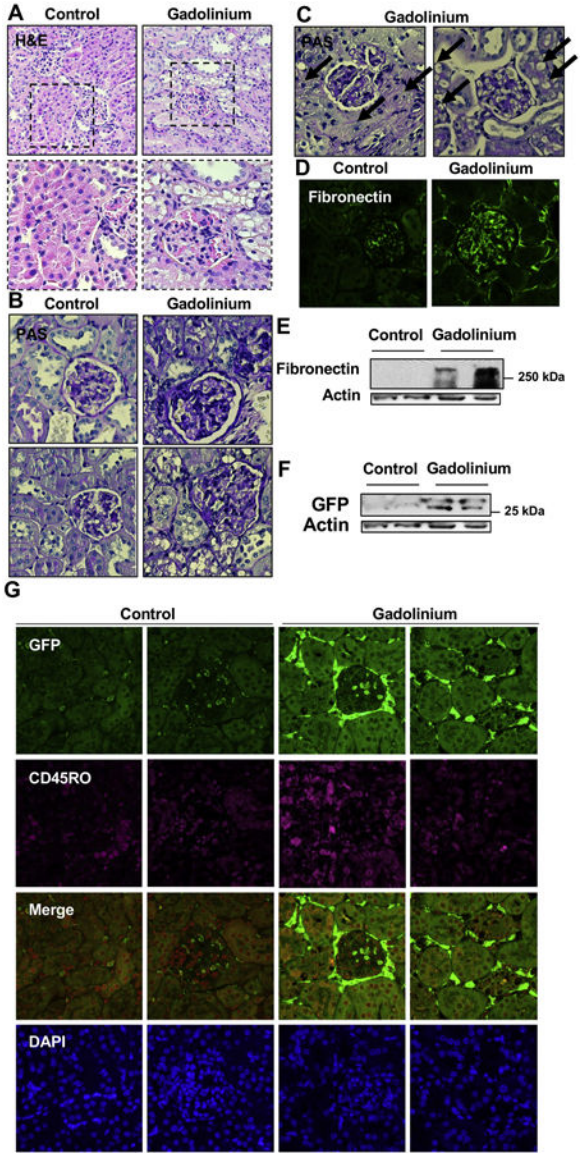

Figure 4.

Gadolinium-based contrast increases myeloid cell infiltration to the kidney. Mice with 5/6th nephrectomies were lethally-irradiated and salvaged with bone marrow transplant from green fluorescent protein-(GFP-) expressing donors. After several weeks of engraftment, mice were treated with gadolinium-based contrast agent 2.5 mmol/kg intraperitoneally daily, 20 doses over 4 weeks. **A.** Proximal tubular vacuolization and glomerulosclerosis, H&E. **B.** Gadolinium increases mesangial matrix and proximal tubular vacuolization. PAS, 400_. **C.** Severe peri-glomerular sclerosis and proximal tubular vacuolization in gadolinium-treated animals. PAS, 400_. **D.** Glomerular fibronectin expression, immunofluorescence, 400_. **E.** Renal cortical fibronectin. Immunoblot. **F.** Expression of the myeloid marker (GFP) in renal cortex. Immunoblot. **G.** Myeloid marker (GFP) and fibrocyte marker (CD45RO) in the glomerulus and renal interstitium. Immunofluorescence, 400_.

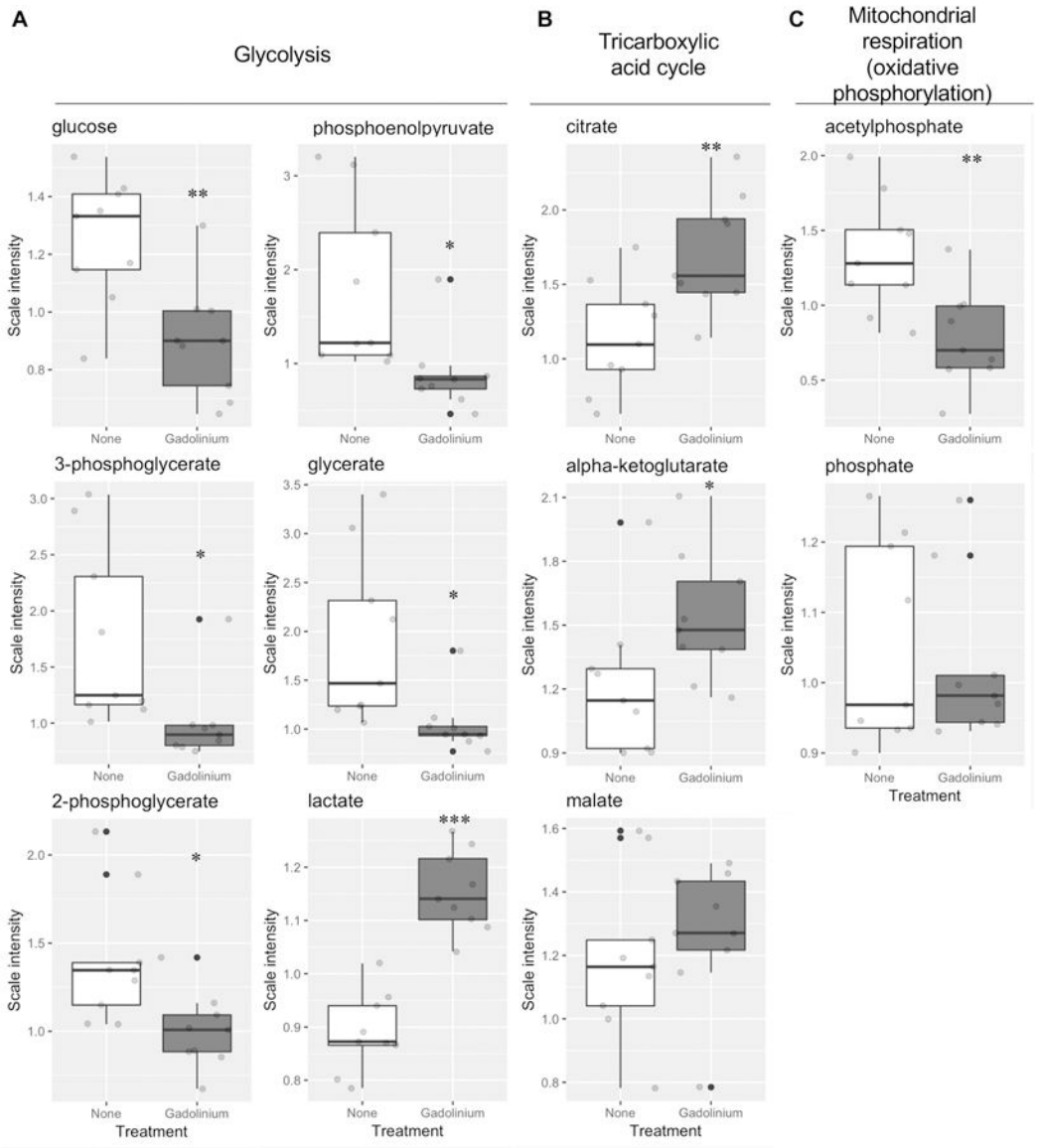

Figure 5.

Gadolinium-based contrast agents are metabolic disruptors. Mice were treated with gadolinium-based contrast agent, 2.5 mmol/kg intraperitoneally, 20 doses over 4 weeks. Metabolites from flash-frozen renal cortex from control and gadolinium-based contrast agent-treated (Gd) animals ($n = 9$ each) were quantified. **A.** Glycolytic pathway. **B.** Tricarboxylic acid (TCA) pathway. **C.** Mitochondrial oxidative phosphorylation (OXPHOS) metabolites. * $P < 0.05$, ** $P < 0.01$, *** $P < 0.001$ by t-test.

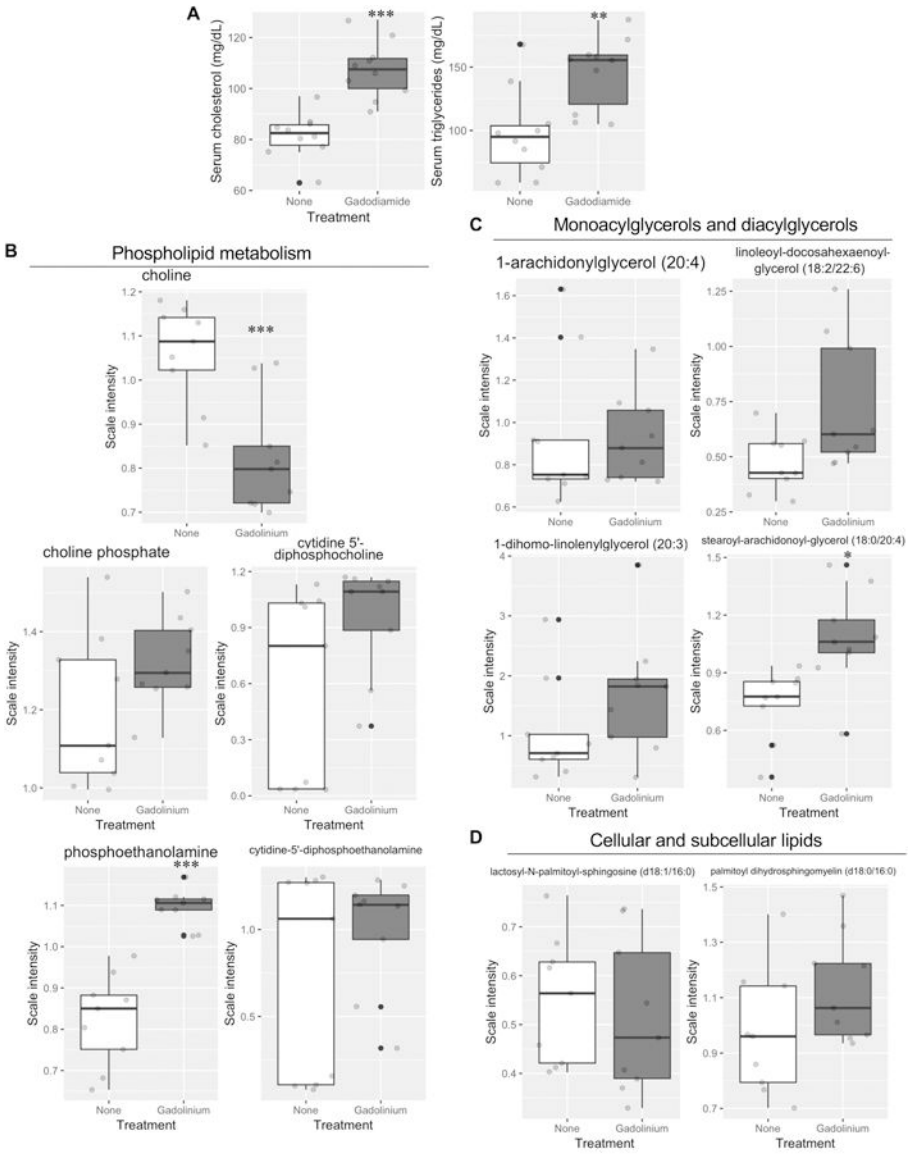

Figure 6.

Gadolinium alters the lipid profile and phospholipid metabolism. **A.** End point serum cholesterol and triglyceride levels. **B.** Monoacylglycerol and diacylglycerol levels. Kidney metabolomic analysis. **D.** Cellular and subcellular membrane constituents, lactoceremides and sphingomyelin. Kidney, metabolomics. * $P < 0.05$, ** $P < 0.01$, *** $P < 0.001$ by *t*-test.

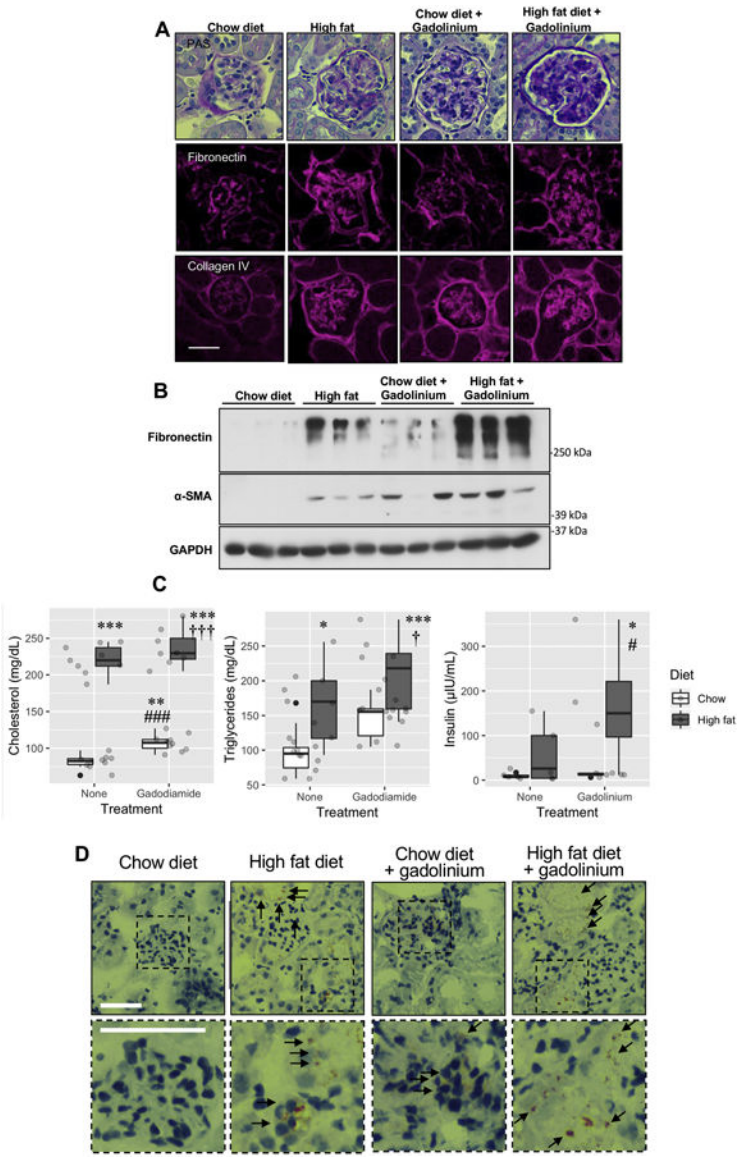

Figure 7.

Obesity amplifies gadolinium-based contrast agent-induced kidney injury. **A.** Renal fibrosis from gadolinium-based contrast agents, obesity, and the combination of the two. Upper panels, PAS, 400 ×. Middle panels, fibronectin. Immunofluorescence, 400×. Lower panels, collagen IV. Immunofluorescence, 400×; calibration bar = 0.05 mm. **B.** Quantitation of fibrotic markers. Immunoblot. **C.** Plasma lipid profiles and insulin levels. * $P < 0.05$, ** $P < 0.01$, *** $P < 0.001$ from untreated, chow diet; # $P < 0.05$, ### $P < 0.001$ from untreated, high-fat diet; † $P < 0.05$, ††† $P < 0.001$ from gadolinium-based contrast agent-treated, chow diet group by analysis-of-variance and Tukey honest significant difference post-hoc testing. **D.** Renal cortex, with arrows indicating lipofuscin-stained cells. Oil red O, 400_, calibration bars = 0.05 mm.

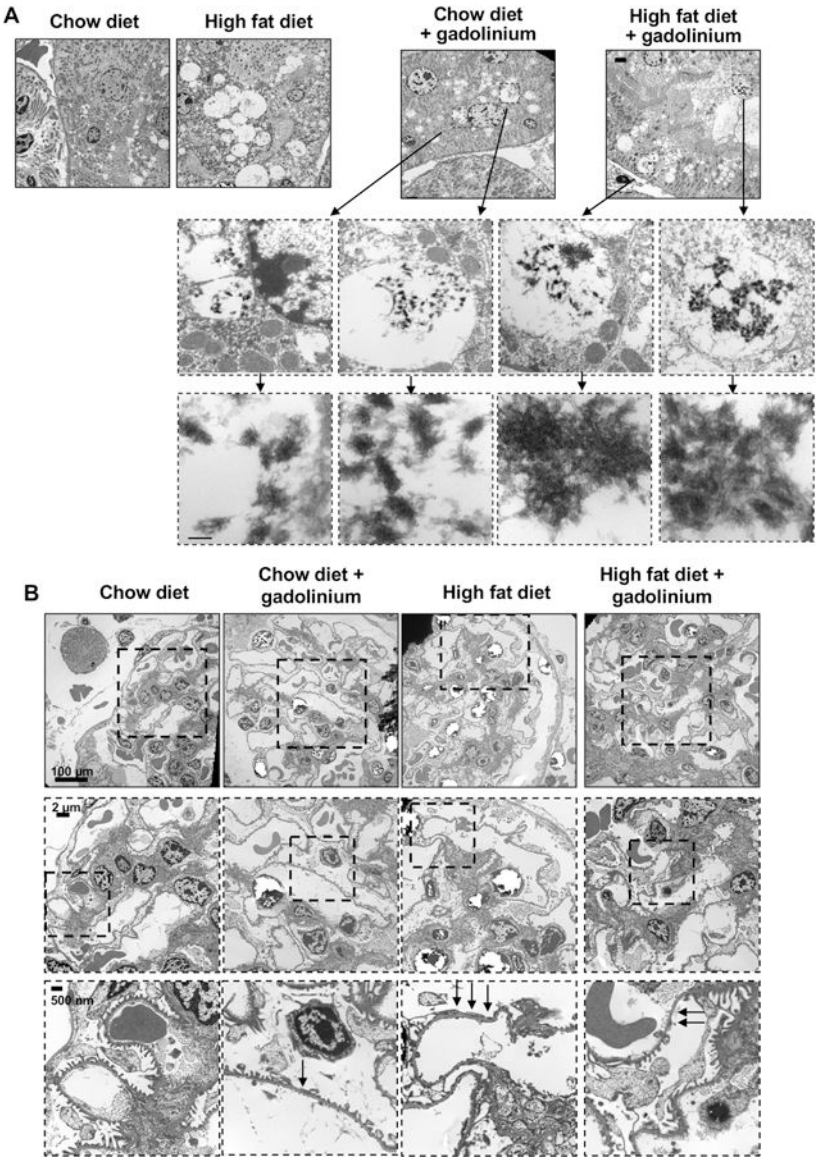

Figure 8.

Renal pathologies induced by gadolinium-based contrast agent treatment, high fat diet-induced obesity, and the combination. **A.** Gadolinium-based contrast agent treatment induces the formation of electron-dense, mesh-like nanowire deposits inside proximal tubular lysosomes (with membranous disruption) *in vivo*. Transmission electron microscopy, calibration bar (top panels) = 2 μm, 100 nm (bottom panels). **B.** Transmission electron microscopy, glomeruli. Arrows indicate the effacement of podocytes. Calibration bars = 100 μm (top panels), = 2 μm (middle panels), = 50 nm (bottom panels).

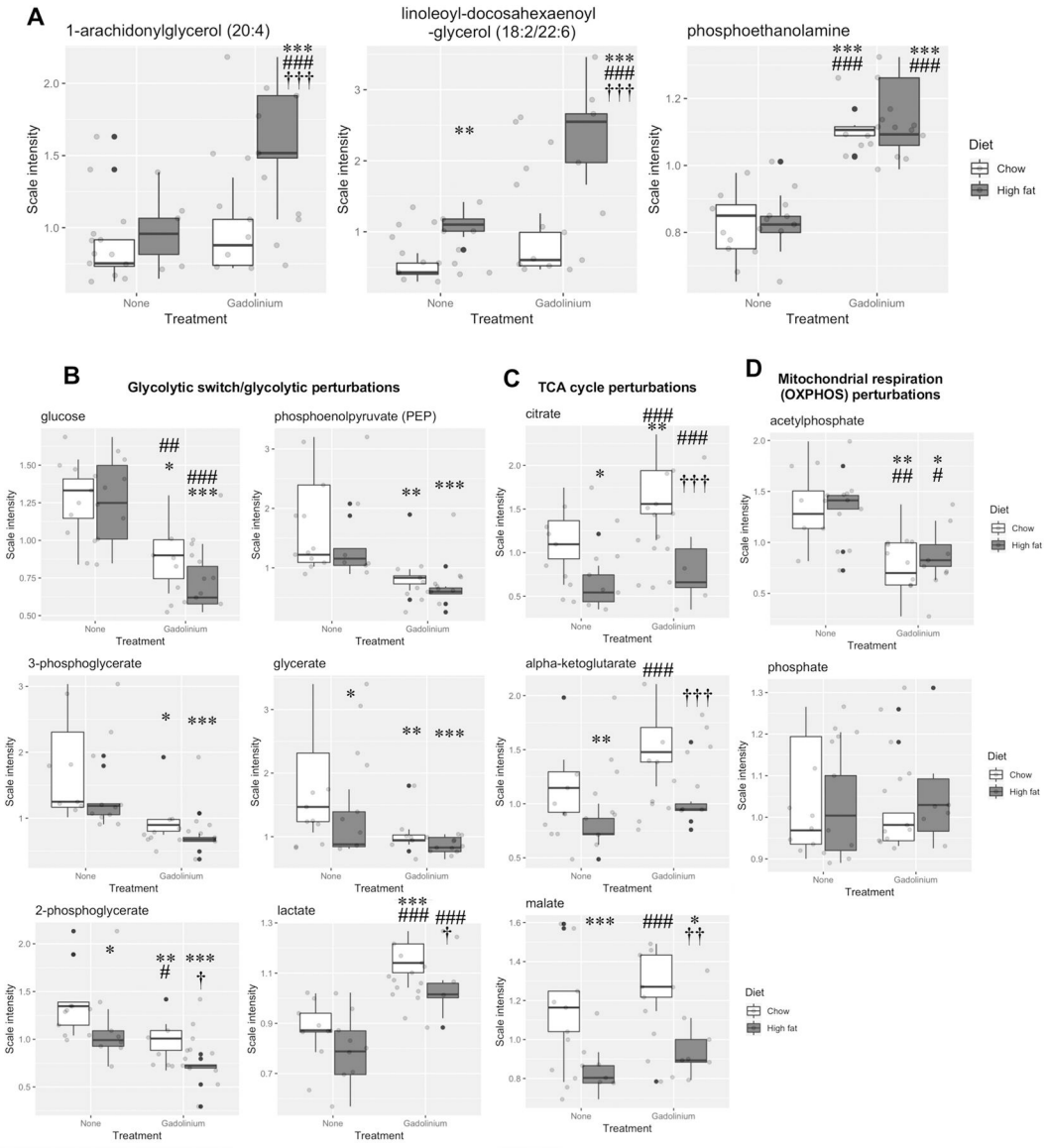

Figure 9.

Renal metabolic impact of gadolinium-based contrast agent treatment, high fat diet-induced obesity, and the combination. **A.** Lipid pathways included monoacylglycerol (1-arachidonylglycerol (20:4)) and diacylglycerol metabolism, (linoleoyl-docohexaenoyl-glycerol (18:2/22:6)), and phospholipid metabolism (phosphoethanolamine).**B.** Impact of gadolinium-based contrast agent, high fat diet-induced obesity, and the combination on kidney glycolysis, the tricarboxylic acid cycle, and mitochondrial oxidative phosphorylation. * $P < 0.05$, ** $P < 0.01$, *** $P < 0.001$ from untreated, chow diet; # $P < 0.05$, ## $P < 0.01$, ### $P < 0.001$ from untreated, high fat diet; † $P < 0.05$, †† $P < 0.01$, ††† $P < 0.001$ from gadolinium-based contrast agent-treated, chow diet by analysis-of-variance with Tukey honest significant difference post-hoc testing.

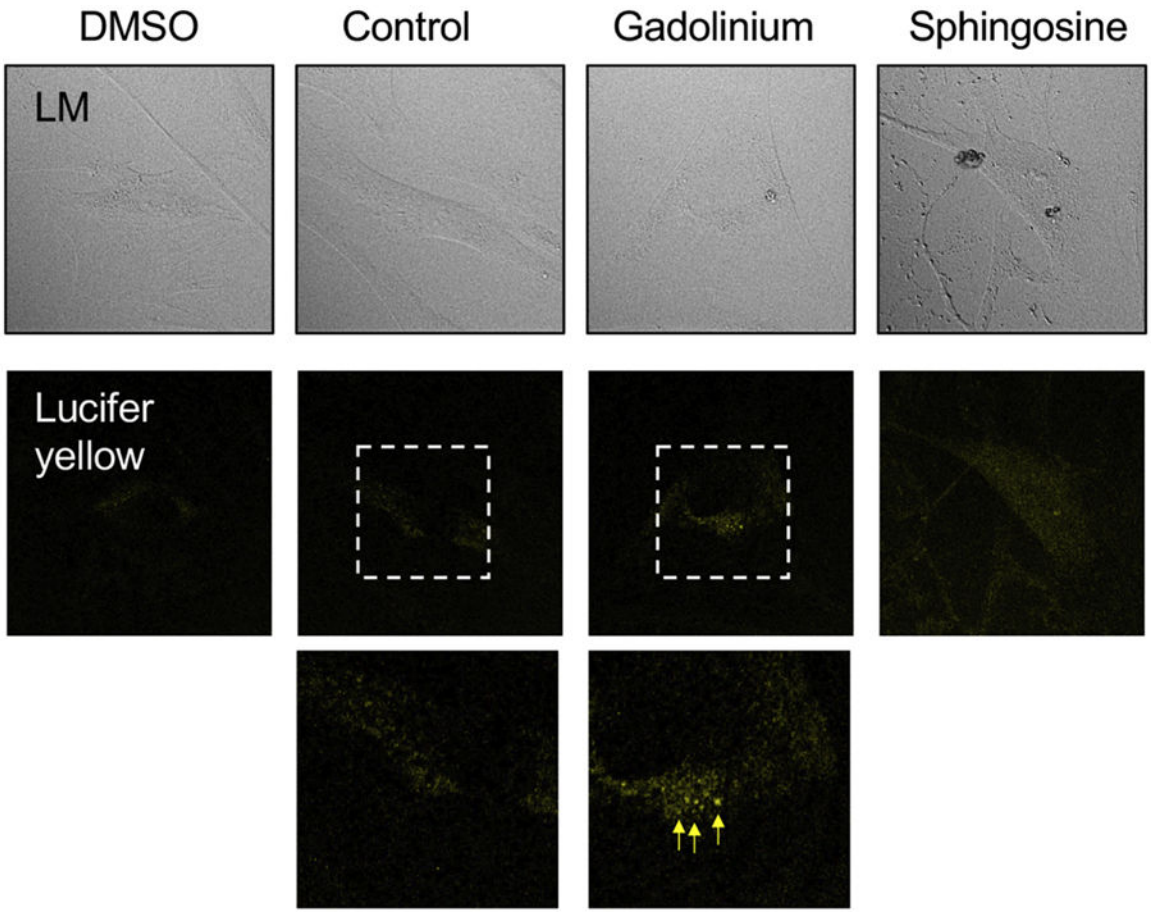

Figure 10.

Impact of gadolinium-based contrast agent treatment on cultured human fibroblasts *in vitro*. Arrows indicate dense, granular lysosomal morphology. Confocal, 40× objective 2× zoom, oil.

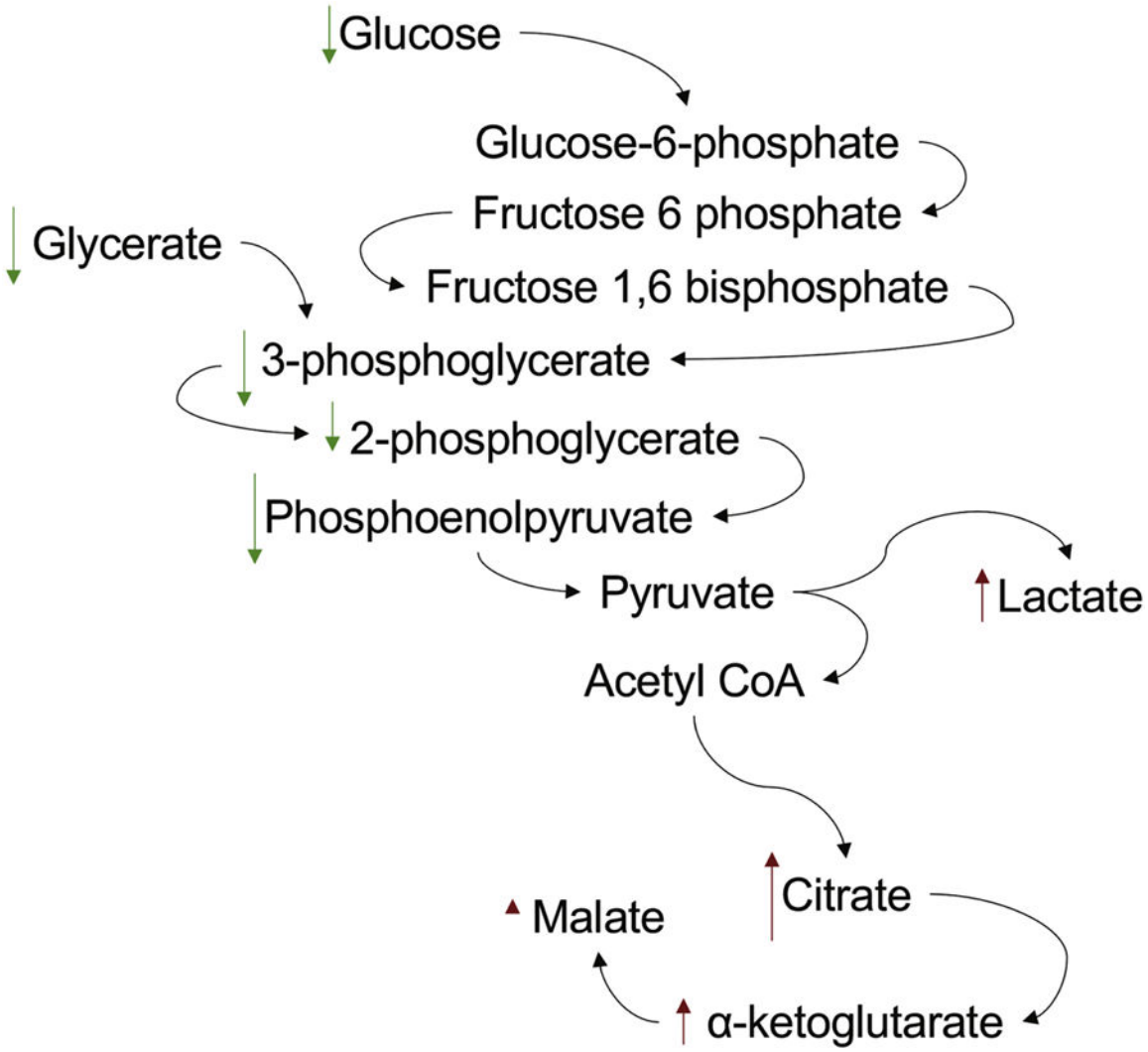

Fig. 11.

Gadolinium-based contrast agent treatment induces the Warburg effect in renal cortex. Magnetic resonance imaging contrast, far from being inert, has a profound impact on increasing glycolysis and the conversion of pyruvate to lactate while decelerating the tricarboxylic acid cycle.

Table 1.

Immunofluorescence stain synopsis

Marker	Dilution	Company	City, State
Green fluorescent protein (ab290)	1:100	Abcam	Cambridge, MA
Collagen IV	1:100	Abcam	Cambridge, MA
Synaptopodin (sc-21536)	1:25	Santa Cruz Biotechnology	Dallas, TX
Fibronectin (F3648)	1:100	Sigma-Aldrich	St. Louis, MO
C-C chemokine receptor 2 (PA523037)	1:100	Thermo Fisher Scientific Life Sciences	Waltham, MA
CD45RO (MA5–11532)	1:25	Thermo Fisher Scientific Life Sciences	Waltham, MA